SILICON ELECTROOSMOTIC MICROPUMPS FOR INTEGRATED CIRCUIT THERMAL MANAGEMENT

Daniel J. Laser[1,3], Alan M. Myers[2], Shuhuai Yao[1], Katrina F. Bell[1], Kenneth E. Goodson[1],
Juan G. Santiago[1], and Thomas W. Kenny[1]
[1]Department of Mechanical Engineering, Stanford University, Stanford, CA 94305
[2]Intel Corporation
[3]Phone - 650.723.0277; Fax - 650.723.3521; email - dlaser@mems.stanford.edu

ABSTRACT

We are developing a class of electroosmotic micropumps fabricated from silicon substrates that can be used for integrated circuit thermal management applications. Prototype micropumps with 0.15 cm^3 packages produce a maximum flow rate of 170 μL min^{-1} and a maximum pressure of 10 kPa operating at 400 V. These specifications approach the requirements for single-phase forced-convective cooling of small IC hot spots. The micropumps operate on less than 200 mW and, having no moving structural elements, offer inherent reliability advantages. The impact on pump performance of geometry, surface treatment, and choice of working fluid has been characterized.

INTRODUCTION

Continued performance improvements for many integrated circuit devices may require new cooling solutions incorporating liquid or two-phase forced convection. Miniature pumps that generate electroosmotic flow using sintered glass frits have been developed to provide two-phase convective cooling for high-power-density integrated circuits [1]. These pumps generate over one atmosphere of pressure at 100 V and can pump liquids at flow rates as high as 33 mL min^{-1}.

Electroosmotic frit pumps produce high pressures and flow rates in high surface-to-volume-ratio structures with sub-micron pores. High-aspect-ratio structures suitable for electroosmotic pumping can also be made using micromachining techniques [2]. In the microfabricated pump shown in Figure 1, narrow slots etched in a silicon substrate form a high surface-to-volume-ratio structure for generating relatively high pressure and flow rate electroosmotic flow. A layer of silicon nitride coats the silicon substrate, providing reliable insulation for operation at up to approximately 500 V. Early prototype micropumps based on this design produced flow rates on the order of 10 μL min^{-1} and pressures on the order of 10 kPa [3].

Since these micropumps have no moving structural elements and are fabricated in a CMOS-compatible process, they may be suitable for IC thermal management applications. One such application is reducing the temperature of small, high-power-density regions of microchips through single-phase forced-convective cooling. Systems-on-a-chip (SoC) and high-performance ICs that contain a mix of high- and low-power devices are prone to developing hot spots during operation. Even with chip-scale heat sinking adequate for the chip's overall power dissipation, the thermal resistance associated with solid-state conduction to the heat sink may be too great to avoid excessive hot spot temperatures. This is particularly true for chips with multiple active layers in a 3-D configuration [4]. A single-phase forced-convection cooling system like the one illustrated in Figure 2(a) is a possible solution. The system incorporates an integrated electroosmotic micropump, avoiding the need for fluidic connections to the chip. Similar systems incorporating arrays of feedback-controlled silicon electroosmotic micropumps could provide on-demand forced convective cooling of spatially- and temporally-varying hot spots.

Zhang et al. showed that a flow rate of 100 μL min^{-1} is sufficient for cooling some hot spots [5]. To estimate the micropump performance requirements for hot spot cooling generally, we use a simple model of a single-phase microchannel heat sink [6]. This model assumes a very small thermal resistance in the solid (Biot number much less than one). Figure 2(b) shows the calculated

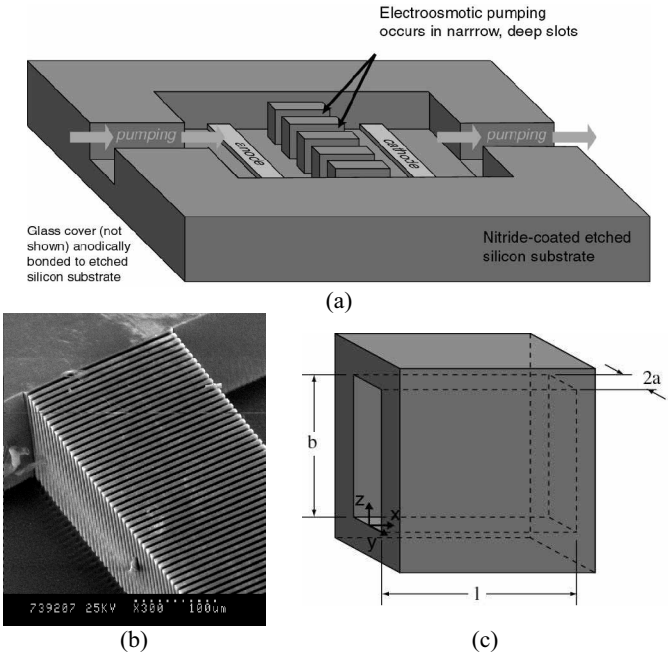

Figure 1. (a) Silicon electroosmotic micropump structure and operation. An axial electric field generates electroosmotic flow in deep, narrow slots plasma-etched into a silicon substrate. A silicon nitride layer passivates the substrate. A cover (glass in the prototypes to allow optical access) is bonded to the silicon to seal the micropump. (b) SEM showing the pumping structure formed by deep etching of silicon. Micropumps with slot widths ranging from 2-4 μm have been fabricated. (c) Notation and coordinate axes used in description and analysis of electroosmotic slot pumps.

0-7803-7731-1/03/$17.00 ©2003 IEEE

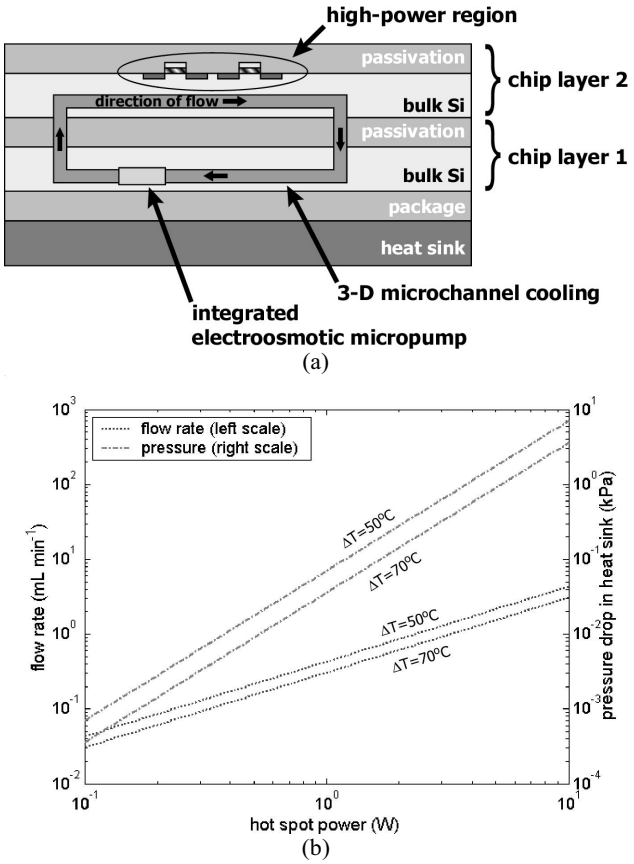

Figure 2. (a) Thermal management system for ICs based on integrated electroosmotic micropumps and microchannels. Single-phase, micropump-driven forced-convective cooling supplements heat conduction from high-power-density regions. In a two-layer 3-D IC, forced convection cools regions on the layer furthest from the heat sink. (b) Estimated flow rate required for single-phase forced-convective cooling of a 1 mm x 1 mm hot spot with a local microchannel heat sink. The pressure drop in the microchannel heat sink is also shown.

flow rate required for single-phase forced-convective cooling of a 1 mm x 1 mm hot spot with a local microchannel heat sink designed to minimize required pumping power. The corresponding pressure drop (across microchannel heat sink) is also plotted. These estimates were made using the properties of water at 30°C and a channel-to-chip cross-sectional area ratio of 0.25. From this analysis, we can conclude that, for an allowed fluid temperature rise of 70°C, forced convective cooling of a 2 W hot spot requires a flow rate of approximately 620 μL min^{-1}. The corresponding pressure drop across the microchannel heat sink is approximately 0.14 kPa. Pressure losses in the rest of the system are estimated at 1-10 kPa. Silicon electroosmotic micropumps for hot spot cooling, therefore, must generate flow rates between one and two orders of magnitude greater than early prototypes while maintaining pressure performance.

DESIGN AND THEORY OF OPERATION

The design variables for electroosmotic micropumps include pump geometry, surface treatment, and the chemistry of the working electrolyte. For an electrooosmotic pump with slot-shaped features (i.e., the geometry shown in Figure 1(c), with $b >> 2a$ and $l >> 2a$) and uniform and constant surface and fluid properties, the flow rate Q that results from applying a uniform axial electrical field E_x is [7, 8]:

$$Q = A\left\{-\mu_{eof} E_x\left[1 - G\left(a/\lambda_D\right)\right] - \phi_1 p_1\right\} \qquad (1)$$

where p_1 is the pressure increase in the pump and A is the total flow cross-sectional area ($A = 2abn$, where $2a$ and b are the cross-sectional dimensions as shown in Figure 1(c) and n is the number of slots). The electroosmotic mobility μ_{eo} and the parameter ϕ_1 are

$$\mu_{eo} = \frac{\varepsilon\zeta}{\mu} \qquad \text{and} \qquad \phi_1 = \frac{a^2}{3\mu l}$$

where μ and ε are the viscosity and permittivity, respectively, of the fluid and ζ is the zeta potential, defined as the potential drop across the diffuse ion region of the electrical double layer. The function G ranges from 0 to 1, depending on the ratio of the slot half-height, a, and the Debye length, λ_D, which is the characteristic thickness of the electric double layer in the region of the liquid/solid interface. We operate our micropumps with weak buffer solutions for which λ_D is of order 100 nm or smaller. These micropumps have slot half-height $a \geq 1$ μm, so finite double layer effects are negligible and $G << 1$. Therefore, flow rate is expected to scale linearly with A and l^{-1} for a given voltage applied across the pumping region.

Viscous losses in the manifolds of silicon electroosmotic micropumps can be significant. Approximating flow in the manifolds of our design with a parallel-plate flow model, the pressure increase from the inlet to the outlet of the pump p_2 is

$$p_2 = -\frac{\mu_{eo}}{\phi_1} E_x\left[1 - G\left(a/\lambda_D\right)\right] - \left(\frac{1}{A\phi_1} + \frac{1}{\phi_2}\right)Q$$

where the parameter ϕ_2 accounts for pressure drops in the manifolds in terms of the effective manifold cross-sectional dimensions a_m and b_m and its length l_m:

$$\phi_2 = \frac{2}{3}\frac{a_m^{\,3} b_m}{\mu l_m}.$$

FABRICATION AND TESTING

Electroosmotic micropumps have been fabricated on 4" silicon wafers in a two-mask process. The slots and manifolds are defined in 7 μm thick photoresist (SPR-220-7) and etched by deep reactive ion enhanced etching. Inlet and outlet ports are then etched from the back side of the wafer. After etching, a layer of near-stoichiometric silicon nitride is deposited at low pressure. A glass cover is then anodically bonded to the nitride-coated wafer to seal the slots and manifolds. The wafer is then diced into individual pumps, platinum wires are inserted into the manifolds through channels running to the sides of the dies, and 0.5 cm long glass tubes are epoxied on to the dies to serve as interconnects. We are also developing

thin-film platinum electrode processes for electroosmotic pumps.

The micropumps described here all have 500 slots spaced at 20 μm intervals, forming a pumping region 1 cm wide. The volume occupied by the pumping regions is less than 1 mm^3. For ease of fixturing (e.g., attaching fluidic interconnects), the micropumps are fabricated on 1.2 cm x 1.3 cm dies. The silicon nitride passivation layer is 400 nm thick. Slot depth b is approximately 70 μm. Micropumps with slot lengths l of 100 μm, 200 μm, and 400 μm were produced. We also fabricated micropumps with an oxide coating on top of the nitride layer. The oxide coating is applied in the high-aspect-ratio slots by performing a short LPCVD polysilicon deposition followed by wet oxidation of the polysilicon layer in its entirety. The slot height $2a$ of oxide-coated micropumps is approximately 2.8 μm; the slot height of the nitride-only micropumps is approximately 2.2 μm.

The silicon electroosmotic micropumps were tested with borate buffer solutions ($Na_2B_4O_7$, pH=9.2) with concentrations (based on Na^+) of 0.2 mM and 0.4 mM. The measured conductivities of these solutions were 15 μS cm^{-1} and 28 μS cm^{-1}, respectively. The micropumps were tested at operating voltages of 200 V and 400 V. Only one of the 22 micropumps tested under these conditions failed due to breakdown of the passivation layer and resultant short-circuiting through the silicon substrate. Flow rate under minimal back pressure conditions was measured by tracking the position of the flow front in an open capillary. Pressure vs. flow rate measurements were performed by measuring compression of a gas column in a closed capillary. The margin of error associated with the open-capillary flow rate measurement technique is approximately 5%; the margin of error for the closed-capillary pressure-flow rate measurement technique is approximately 15%. Current was monitored during tests by observing the voltage drop across a small reference resistor in series with the micropump. The margin of error associated with this measurement technique is approximately 15%. Some variation in micropump performance was observed from day to day and over the course of repeated testing during a particular day. This variability is currently under investigation. The data reported here is from micropumps that had been allowed to stand for at least three days between tests.

RESULTS AND DISCUSSION

Figure 3 shows pressure, as a function of flow rate, generated at 200 V and 400 V by micropumps with 100 μm long oxide-coated pumping regions. Pressure-flow rate results where repeatable within +/- 30% for multiple tests of the same micropump and for tests of different micropumps with the same geometry and surface. Measured power consumption was approximately 150 mW at 400 V and 40 mW at 200 V. Thermodynamic efficiency is approximately 0.05%. Zeta potential, estimated from the maximum generated pressures using (1) above, was found to be between –20 and –25 mV. Streaming potential measurements are currently being performed to better characterize the zeta potential of the micropump surfaces.

Micropumps with 100 μm, 200 μm, and 400 μm long pumping regions (in the flow direction) were tested under minimal-back-pressure conditions at 200 V with 0.2 mM and 0.4 mM buffers. The electric field in the pumping region was estimated with a one-dimensional model to account for potential drops in the manifolds. The measured maximum flow rates Q_{max} scaled by the electric field in the pumping region produced by pumps of each

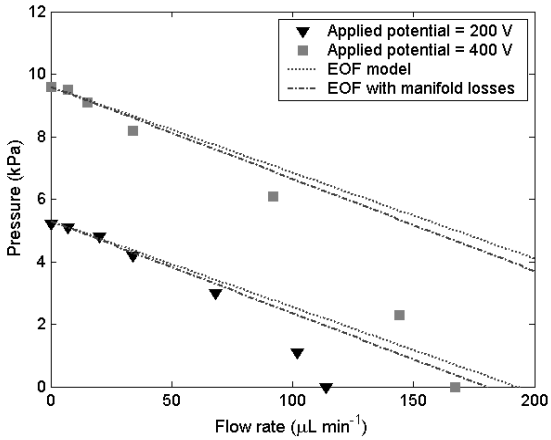

Figure 3. Pressure-flow rate performance of silicon electroosmotic micropumps with 100 μm long oxide-coated pumping regions. The working fluid is 0.2 mM borate buffer. Zeta potential is calculated based on the maximum generated pressure and used to determine the expected pressure vs. flow rate relationship for the micropump geometry.

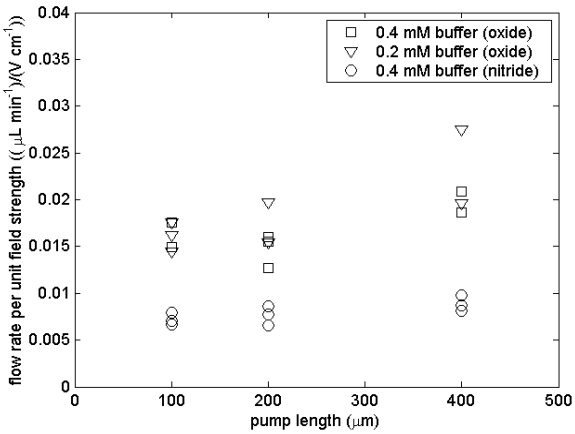

Figure 4. Flow rate per unit electric field strength generated by silicon electroosmotic micropumps. All tests performed at 200 V with minimal back pressure. Tests of micropumps with oxide-coated pumping surfaces revealed no discernable dependence of flow rate on electrolyte concentration for 0.2 mM and 0.4 mM buffers. Micropumps with shorter pumping regions produce higher absolute flow rates, but flow rate per unit field strength is generally independent of pumping region length. Micropumps with oxide-coated pumping surfaces produce substantially higher flow rates than those with bare silicon nitride pumping surfaces.

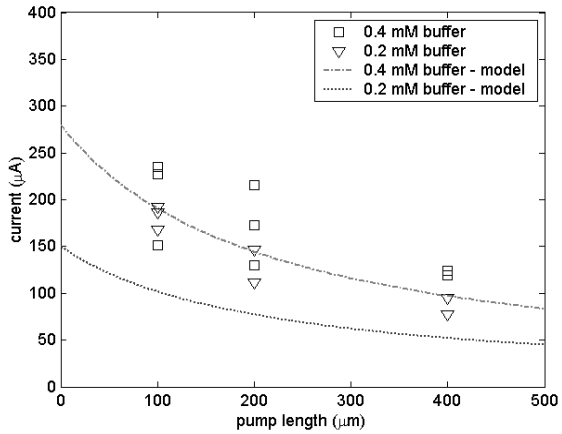

Figure 5. Measured current through the silicon electroosmotic micropumps during operation at 200 V. Electromigration current (calculated based on the micropump geometry and measured buffer conductivity) is also shown.

length is shown in Figure 4. As expected, flow rate per unit applied field is generally independent of pump length. No dependence of performance on buffer concentration was discernable for the two buffer concentrations used. Micropumps with oxide-coated pumping surfaces consistently produced higher Q_{max} than those with bare nitride pumping surfaces.

Figure 5 shows the measured current drawn by the micropumps during operation at 200 V against minimal back pressure. Also shown is the current expected to result from electromigration in the micropumps during operation. The electromigration current is predicted from the micropump geometry and the measured bulk buffer conductivity.

Relative to their size, the flow rate produced by the silicon electroosmotic micropumps exceeds that of many reciprocating displacement micropumps that require more complex fabrication processes. Pressure generation is comparable to that of many reciprocating displacement micropumps. Measured micropump performance was generally consistent with models for electroosmotic flow. Some variation in micropump performance for low buffer concentration experiments may be due to unstable pH conditions. Also, at very low concentrations, ionic impurities from surfaces and gases in contact with the buffer (e.g., carbonic acid resulting from CO_2-water reactions) can have a significant impact on buffer conductivity. At times, measurements of buffers conductivity several hours or days after preparation revealed significant deviation (+/- 25%) from the nominal values. This was particularly the case for the 0.2 mM buffer. The micropumps were also tested with buffers at concentrations below 0.2 mM, but conductivity (and performance) variations with these buffers were so great that the tests were discontinued. Operating at concentrations below 0.2 mM, while desirable from the standpoint of maximizing micropump efficiency, is impractical. Operating at 200 V with 0.2 mM and 0.4 mM buffers, the micropumps consume less than 50 mW.

CONCLUSIONS

Silicon electroosmotic micropumps for integrated circuit thermal management applications have been fabricated and extensively tested. Reducing the length of the pumping region and coating the pumping surfaces with silicon oxide has been shown to significantly improve micropump performance. Micropumps with 100 μm long pumping regions and oxide-coated pumping surfaces produce a maximum flow rate and pressure of 170 μL min^{-1} and 10 kPa, respectively, at 400 V. This flow rate is more than an order of magnitude higher than that produced by earlier prototypes. Additional design refinements are expected to elevate silicon electroosmotic micropump performance to the level required for forced convective cooling of IC hot spots.

ACKNOWLEDGEMENTS

This work is supported by Intel Corporation and by the Semiconductor Research Corporation Graduate Fellowship Program. We made use of National Nanofabrication Users Network facilities funded by the National Science Foundation under award ECS-9731294.

REFERENCES

1. Yao, S., et al., *Porous Glass Electroosmotic Pumps.* Submitted to Journal of Colloid and Interface Science.

2. Chen, C.-H. and J.G. Santiago, *A Planar Electroosmotic Micropump.* Journal of Microelectromechanical Systems, 2002. **11**(6): p. 672-683.

3. Laser, D.J., et al. *High-Frequency Actuation with Silicon Electroosmotic Micropumps*. *2002 Solid State Sensors and Actuators and Microsystems Workshop*, 2002, Hilton Head, S.C.

4. Banerjee, K., et al., *3-D ICs: A Novel Chip Design for Improving Deep-Submicrometer Interconnect Performance and Systems-on-Chip Integration.* Proceedings of the IEEE, 2001. **89**(5): p. 602-633.

5. Zhang, L., et al., *Measurements and modeling of two-phase flow in microchannels with nearly constant heat flux boundary conditions.* Journal of Microelectromechanical Systems, 2002. **11**(1): p. 12-19.

6. Murakami, Y. and B.B. Mikic, *Parametric Optimization of Multichanneled Heat Sinks for VLSI Cooling.* IEEE Transactions on Components and Packaging Technologies, 2001. **24**(1): p. 2-9.

7. Hunter, R.J., *Zeta Potential in Colloid Science*. 1981, San Diego: Academic Press, Inc.

8. Burgreen, D. and F.R. Nakache, *Electrokinetic Flow in Ultrafine Capillary Slits.* J. Phys. Chemistry, 1964. **68**(5): p. 1084-1091.